https://doi.org/10.3799/dqkx.2022.236

激光拉曼光谱仪定量测定硅酸盐熔体包裹体中水含量及其地质应用

高晓英[1,2],涂 聪[1],孟子岳[1]

1. 中国科学技术大学地球和空间科学学院,中国科学院壳幔物质与环境重点实验室,安徽合肥 230026
2. 中国科学院比较行星学卓越创新中心,安徽合肥 230026

摘 要: 水作为深熔熔体中最常见的一种挥发分,是影响熔体的物理和化学性质的主要因素.由于现有的测试技术以及熔体包裹体自身的局限性,很难定量确定熔体包裹体中水的含量和种型,导致对俯冲带熔体产生机制和演化过程的认识也极为有限.共聚焦显微激光拉曼光谱仪具有高的空间分辨率、快速、无损分析、样品制备简单等优点,且可分析暴露于表面或包裹于内部的样品,因此对探测微小熔体包裹体具有极大的优势.该方法的原理是基于拉曼谱峰高度/强度与其对应基团含量具有良好的线性关系,以人工合成硅酸盐玻璃为标准样品,用于硅酸盐熔体包裹体中水的含量和种型的定量限定.作为新发展起来的技术和方法,越来越多地引起地质学家的关注,但是目前大量的研究还集中于该分析方法自身的推演和校正,对天然样品的研究还相对缺乏.目前有限的研究表明,该方法可被广泛应用于岩浆岩和高级变质岩体系中,不仅可定量限定岩浆岩基质或斑晶中硅酸盐熔体包裹体水含量,有效示踪岩浆侵入或喷发过程中岩浆的流变学行为;而且可定量限定俯冲带内经历过部分熔融的高级变质岩中代表初始熔体的多晶矿物包裹体中水的含量和种型,示踪俯冲带熔体组成和演化,进而为研究深俯冲地壳分异、板片-地幔楔界面的熔体交代作用等重要问题提供新的制约.

关键词: 水;拉曼光谱;硅酸盐玻璃;熔体包裹体;碰撞造山带;地球化学.

中图分类号: P574.2 **文章编号:** 1000-2383(2022)10-3616-17 **收稿日期:** 2022-03-28

Geological Application of Raman Spectroscopy to Quantify Trace Water Concentrations in Silicate Glasses

Gao Xiaoying[1,2], Tu Cong[1], Meng Ziyue[1]

1. *School of Earth and Space Sciences, University of Science and Technology of China; Key Laboratory of Crust-Mantle Materials and Environments, Chinese Academy of Sciences, Hefei* 230026, *China*
2. *Chinese Academy of Sciences Center for Excellence in Comparative Planetology, Hefei* 230026, *China*

Abstract: Water, the primary volatile constituent in anatectic melt and terrestrial magma, has a significant effect on the physical and chemical properties of the melt. Due to limitations in analytical techniques and the fugitive nature of anatectic melts, it is extremely difficult to quantitatively determine water concentration and water speciation, resulting in a very limited understanding of the formation mechanism and evolution process for partial melting in subduction zone. Confocal micro-Raman spectroscopy, which has the advantages of high spatial resolution, fast, nondestructive analysis and simple sample preparation, severs the

基金项目: 国家自然科学基金项目(No. 42072070);中央高校基本科研业务费专项资金资助(No. WK2080000128).

作者简介: 高晓英(1980-),女,教授,主要从事大陆俯冲带矿物学和岩石地球化学研究. ORCID: 0000-0002-6624-6092. E-mail: gaoying@ustc.edu.cn

引用格式: 高晓英,涂聪,孟子岳,2022.激光拉曼光谱仪定量测定硅酸盐熔体包裹体中水含量及其地质应用.地球科学,47(10):3616-3632.

Citation: Gao Xiaoying, Tu Cong, Meng Ziyue, 2022. Geological Application of Raman Spectroscopy to Quantify Trace Water Concentrations in Silicate Glasses. *Earth Science*, 47(10): 3616-3632.

purpose of detecting small melt inclusions. Additionally, based on the principle that there is a good linear relationship between the height/intensity of Raman spectrum peak and the content of corresponding groups, the internal calibration and external calibration are established for the quantitative analysis of water content and water speciation in silicate melt inclusions with synthesized silicate glass as the standard sample. As a newly developed technique and method, more and more geologists pay attention to it. However, a large number of researches are still focused on the deduction and correction of the analytical method itself, while the research on natural samples is relatively lacking. Limited research indicates that the method can be widely used in magmatites and high-grade metamorphic rocks. It achieves quantitatively determining the water content of matrix or melt inclusion in porphyry, thereby effectively tracing the rheological behavior of magma during magma intrusion or eruption. Water content and speciation of the anatectic melt in the continental subduction zone provides tight constraints for continental crust differentiation and melt metasomatites at the slab-wedge interface.

Key words: water; Raman spectroscopy; silicate glass; melt inclusion; collisional zone; geochemistry.

0　引言

俯冲带水的分布和循环,可以显著地影响岩石体系(包括矿物、岩石,乃至于熔体)的物理和化学性质(Mackwell *et al.*, 1985; Karato, 1990, 2010; Hier-Majumder *et al.*, 1997; Mei and Kohlstedt, 2000; Hofmeister, 2004; Yoshino *et al.*, 2006; Hui and Zhang, 2007; Zhang *et al.*, 2010; Ni *et al.*, 2011),影响板内地震(Hacker *et al.*, 2003; Zhang *et al.*, 2004)、地幔对流(Hirth and Kohlstedt, 2003)、地球化学循环(Zack and John, 2007; Shaw *et al.*, 2008; Kelley *et al.*, 2010)等俯冲带重要的物理和化学过程,最终影响地球的长期热和化学演化.因此有人认为,没有水,板块运动就不会发生,就不会形成现在宜居的星球(Regenauer-Lieb *et al.*, 2001).

深熔熔体作为俯冲带里水的重要载体,是板块构造研究的一个重要组成部分(Zheng *et al.*, 2011; Grove *et al.*, 2012).水的存在可以促进矿物反应,诱导岩石体系发生熔融,催化变质反应进行.此外俯冲板块内部存在的深熔熔体活动,可以引起元素和同位素变化,对造山带的构造热演化、俯冲带折返动力学机制、壳幔相互作用和地壳物质再循环等具有重要影响(Rosenberg and Handy, 2005; Zheng, 2009, 2019; Beaumont *et al.*, 2010; Labrousse *et al.*, 2011; Zheng and Hermann, 2014; 郑永飞和陈伊翔, 2019; Wang *et al.*, 2021).大陆俯冲带广泛分布的高压－超高压岩石中的部分熔融作用可以强烈影响大陆地壳的热力学和流变学行为,是花岗质岩浆形成、造山带演化和大陆地壳分异的重要机制(Brown and Rushmer, 2006; Brown, 2013; Zheng and Gao, 2021).

水作为熔体中最常见的一种挥发分,通常有结构羟基(OH)和分子水(H_2O)两种形式,并且两者之间可以相互转换(Wallace, 2005; Zhang *et al.*, 2010; Ni *et al.*, 2011),是影响熔体的物理和化学性质的主要因素之一.它能够不同程度上决定熔体的粘度、密度、热容比、元素扩散速率等物理化学参数(Giordano *et al.*, 2008; Zhang *et al.*, 2010; González-García *et al.*, 2018, 2019).在岩浆体系中,H_2O的增多可以导致岩浆粘度降低致使岩浆流动性增强,并且影响潜热的释放,延长岩浆房寿命(Lee Cin-Ty *et al.*, 2015; Ni *et al.*, 2016);在部分熔融过程中,H_2O的存在可以降低岩石体系的熔融温度,影响熔融程度,加快变质反应进行,影响熔体活动(Zheng *et al.*, 2011; 高晓英, 2019).因此对熔体包裹体中H_2O含量的研究,有助于识别熔体性质和熔融机制,对于花岗岩成因及大陆地壳分异具有重要的指示意义(Thomas, 2000; Thomas *et al.*, 2006, 2008; Bartoli *et al.*, 2013a; Brown, 2013; Ferrero *et al.*, 2015, 2016; Zheng and Gao, 2021).

由于深熔熔体极不稳定且容易挥发,通常会受到后期地质作用的影响,而由于现有技术很难在较深的地幔/地壳条件下直接测定其熔体相(Zhang *et al.*, 2008; Zheng *et al.*, 2011),这也导致对俯冲带熔体产生机制和演化过程的认识极为有限.现有的研究表明,在岩浆形成演化过程中,早期结晶矿物能够捕获体系中的熔体而形成熔体包裹体,通过对熔体包裹体的研究可以探究天然岩浆的物理化学性质、岩浆成矿过程、花岗岩形成和演化等重大地质事件(Sorby, 1858; Frezzotti, 2001; Thomas and Davidson, 2012; Tacchetto *et al.*, 2018).在变质深熔作用过程中,不同类型的熔体包裹体在转熔矿物中被发现,如在高压－超高压变质岩石(如大别－苏鲁榴辉

岩、片麻岩；Zeng *et al.*, 2009; Gao *et al.*, 2012, 2013, 2017; Liu *et al.*, 2013, 2020; Wang *et al.*, 2014, 2017)和高温—超高温变质岩石中均有发现(如印度Kerala Khondalite造山带麻粒岩；Cesare *et al.*, 2009, 2011; Groppo *et al.*, 2012; Ferrero *et al.*, 2012, 2014; Darling, 2013; Bartoli *et al.*, 2013b, 2015, 2016).这些深熔熔体通常被转熔矿物所捕获形成熔体包裹体,在后期冷却结晶过程中形成硅酸盐玻璃包裹体或多相晶体包裹体(简称,多晶包体).这些熔体包裹体被矿物捕获后,可以保持封闭而不受后期过程的影响,因此在重建和恢复早期岩浆/深熔熔体时更为可靠,尤其在直接确定其挥发分含量和性质方面具有独特优势.

近年来,关于俯冲带变质岩中熔体包裹体的研究大多集中于限定其形貌、结构、矿物主微量元素组成等(Zeng *et al.*, 2009; Ferrero *et al.*, 2012, 2014; Gao *et al.*, 2012, 2014, 2017; Liu *et al.*, 2013, 2020; Chen *et al.*, 2014),由于大部分熔体包裹体组分极不均一,且体积较小(<15 μm),所以很难准确限定其化学组成(Halter *et al.*, 2002; Bartoli *et al.*, 2013a; Gao *et al.*, 2013),为了避免因成分不均一而导致的复杂测试过程和测试误差,部分研究者尝试利用活塞圆筒压机在高温高压条件下对多晶的熔体包裹体进行均一化实验,进而准确限定熔体中的主量元素(Malaspina *et al.*, 2006; Bartoli *et al.*, 2013a; Cesare *et al.*, 2015; Ferrero *et al.*, 2015).然而由于现有的测试技术以及熔体包裹体的自身局限,很难准确定量确定熔体包裹体中水的含量和种型,导致对俯冲带熔体产生机制和演化过程的认识也极为有限.因此,包裹在转熔矿物(如石榴子石、绿辉石等矿物)中的天然熔体包裹体是深俯冲大陆地壳深熔的最直接证据,也成为探索地壳深熔作用、花岗岩形成机制、极端变质作用、大陆地壳形成和演化等重大科学问题的理想研究对象(Zeng *et al.*, 2009; Gao *et al.*, 2012, 2013, 2014, 2017; Cesare *et al.*, 2015; Ferrero *et al.*, 2015, 2016, 2018).

1 定量限定水含量方法及其优缺点

随着科学技术的飞速发展,科学家们也先后开发利用不同的方法来定量测定硅酸盐玻璃熔体中的水含量,主要包括全岩粉末和微区原位分析两种.但是不同的方法侧重点不同,其对样品制备以及数据的准确性都存在着较大的差别.全岩粉末分析方法包括Karl Fisher滴定法(KFT)、热重法(TG)、热分解元素分析仪—质谱联机(TC/EA-MS)等(Chen *et al.*, 2007, 2011; Gong *et al.*, 2013),这些方法虽然具有较高的精确度,但是无法对样品进行原位分析.由于熔体包裹体通常具有较小的尺寸(通常<15 μm,大部分集中在5～10 μm),且较难从寄主矿物中分离出来,使得常规测量岩石和矿物中水含量的方法失效.

随着原位微区分析技术的飞速发展,仪器的灵敏度和精确度已有显著提高,涌现出了包括二次离子(SIMS)、傅里叶转换红外光谱(FTIR)、电子探针(EMP)和激光拉曼光谱(Laser Raman Spectra)等分析技术来定量测试熔体包裹体中的水含量.(1)离子探针具有高精度(>1%)和相对高的空间分辨率(～15 μm)的优势,但往往受制于分析标样的选择和建立,分析成本较高,且只能分析样品表面已暴露部分的水含量(Deloule *et al.*, 1995; Hauri *et al.*, 2002; Leschik *et al.*, 2004; Di Muro *et al.*, 2006a, 2006b; Thomas *et al.*, 2006);(2)红外光谱仪由于具有较高精度和高灵敏度(～10×10^{-6})的优点而受到广泛关注,是目前较为常用的原位测试矿物中水含量的方法(Stolper, 1982; Newman *et al.*, 1986; Silver *et al.*, 1990; Withers and Behrens, 1999; Ohlhorst *et al.*, 2001; Mandeville *et al.*, 2002).但是该方法却受制于严苛的样品制备,待测样品需暴露表面且需双面抛光.同时红外光谱仪的空间分辨率较低(分析束斑通常30～50 μm),无法满足微小样品的分析.此外,对于包裹于透明矿物内部的熔体包裹体,只能使用透射模式进行测定,然而在此模式下必然存在寄主矿物对红外光谱的吸收干扰进而导致测试出现偏差,因此无法测试俯冲带陆壳岩石中的细小熔体包裹体;(3)电子探针虽然具有相对高的空间分辨率(～1～5 μm),但是对于水含量的限定是通过分析测试熔体包裹体主量元素含量(包括S、Cl和F),并将它们的总和与100%的差值相扣除作为熔体包裹体中的水含量(Devine *et al.*, 1995; Morgan and London, 1996; Berndt *et al.*, 2005),该方法中的水含量是间接估算而得,严格来说存在较大误差;(4)相较于其他原位分析方法来说,共聚焦激光拉曼光谱仪由于具有较高的空间分辨率(～1～2 μm,性能良好者可达0.5 μm)、高精度(±0.25%)、高灵敏度、快速、无损、

样品制备极其简单等优点,且既可分析暴露于表面的样品也可分析包裹于内部的样品.虽然共聚焦激光拉曼光谱仪对硅酸盐熔体中的水含量具有相对较低的检出限(>0.1%,即>1 000×10^{-6}),但基于其他方面的优势,因此,被成功应用于定量测试矿物内部的熔体包裹体(McMillan and Hofmeister, 1988; Ihinger *et al.*, 1994; Chabiron *et al.*, 1999; Thomas, 2000, 2002; Di Muro *et al.*, 2006a, 2006b; Thomas *et al.*, 2006, 2008; Mercier *et al.*, 2009; Schiavi *et al.*, 2018; Bodnar and Frezzotti, 2020).目前,共聚焦激光拉曼光谱仪定量限定熔体包裹体中的水含量方法一经提出和建立(Thomas, 2000, 2002),立即引起国内外地质学家的广泛关注并被成功应用于花岗岩、伟晶岩、地幔橄榄岩和不同类型的深熔变质岩中熔体包裹体,包括玻璃质包裹体(Thomas *et al.*, 2006, 2008)或均一化的多晶包裹体(Bartoli *et al.*, 2013a; Ferrero *et al.*, 2015, 2016)的研究,且成功获得了熔体包裹体中的水含量,限定了俯冲带熔流体的性质和行为,为大陆地壳形成和演化提供了重要的制约(Zajacz *et al.*, 2005; Di Muro *et al.*, 2006a; Bartoli *et al.*, 2013a; Schiavi *et al.*, 2018; González-García *et al.*, 2020).

2　激光拉曼光谱仪定量限定硅酸盐玻璃水含量的基本原理

共聚焦激光拉曼光谱仪是基于拉曼散射效应的一种光谱分析方法.由于不同样品具有不同的结构(主要体现在化学键的不同和同一化学键的振动方式不同),当入射光照射至样品表面会激发产生具有典型特征的拉曼位移(简称频移),且当实验条件不变时,拉曼散射光的通量与单位体积内的分子数成正比,具体表现在拉曼光谱谱峰高度/谱峰面积与其对应的基团的含量呈线性关系,因此被广泛应用于物质分子结构的定性或定量研究.当入射激光照射至含水的硅酸盐玻璃(包括人工合成的硅酸盐玻璃和天然的熔体包裹体)表面时,会发生非弹性散射,可激发出其内的官能团拉曼谱峰,水的谱峰主要集中在~3 300~3 600 cm^{-1},并且该谱峰高度/谱峰强度(即谱峰积分面积)与其水含量具有良好的线性相关性(图1; McMillan and Hofmeister, 1988; Thomas, 2000, 2002; Zajacz *et al.* 2005; Thomas *et al.* 2006),基于此,建立了外标法和内标法两种定量标定硅酸盐玻璃中的水含量的方法(Thomas, 2000; Chabiron *et al.*, 2004; Zajacz *et al.*, 2005; Behrens *et al.*, 2006; Le Losq *et al.*, 2012).

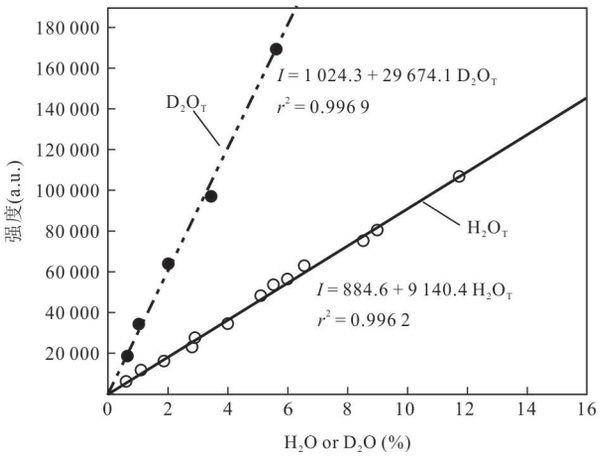

图1　合成含水硅酸盐玻璃的水含量(H_2O或D_2O)与拉曼积分面积的相关性(修改自 Thomas *et al.*, 2006)

Fig. 1　Correlation between H_2O and D_2O concentrations in synthetic glasses and the integral intensity (modified after Thomas *et al.*, 2006)

含水硅酸盐玻璃的激光拉曼光谱显示出多段式特征谱峰(图2):(1)位于低频区间硅氧Si(Al)-O键振动所引起的400~1 250 cm^{-1}峰段,该区内由两个主要峰段400~700 cm^{-1}(Low Frequency, 简称LF)和800~1 200 cm^{-1}(High Frequency,简称HF)组成.LF主要由四面体内T-O-T(T代表4次配位的Si^{4+}、Al^{3+})的连接引起,其中位于LF段~500 cm^{-1}的峰(LF_{500})主要由硅氧四面体桥氧键(T-O-T)的弯曲振动和摆动引起;HF段~1 000 cm^{-1}的峰(LF_{1000})主要由硅氧四面体中非桥氧键(T-O)的伸缩振动引起,该峰强与硅氧四面体中非桥氧的数量有关(Mysen *et al.*, 1980; Sharma *et al.*, 1981; Mysen *et al.*, 1982; McMillan, 1984);(2)位于高频区间3 000~4 000 cm^{-1}的峰段,主要反映的是全水(H_2O_T)峰段,其峰位主要集中在~3 550 cm^{-1},由水分子H_2O_m和羟基水O-H伸缩振动引起(McMillan and Remmele, 1986; Mysen *et al.*, 1997).拉曼全水峰段通常可被分解成若干个高斯或高斯+洛伦兹类型的子峰,在定量标定全水含量的基础上,同时还可以运用子峰定量估算不同种型水的含量,包括水分子H_2O_m和羟基水O-H的相对含量(Mysen and Virgo 1986a, 1986b; Chabiron *et al.*, 2004; Behrens *et al.*, 2006; Di Muro *et al.*, 2006a,

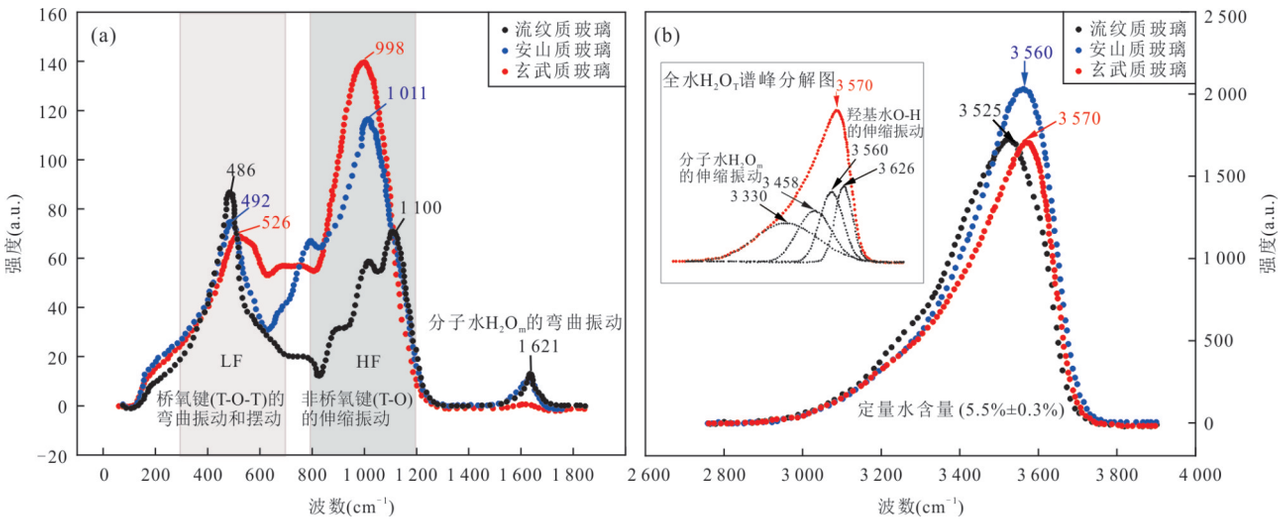

图 2 含水硅酸盐玻璃激光拉曼光谱图(修改自 Zajacz *et al.*, 2005)

Fig. 2 Effect of the chemical composition of the glass on the water band shape (modified after Zajacz *et al.*, 2005)

a. 低频区硅氧 Si(Al)-O 键的振动;b. 高频区全水 H_2O_T 的伸缩振动

2006b);(3)在中频区~1 620 cm^{-1}附近,也出现有微弱的由分子水 H_2O_m 弯曲振动所引起的谱峰(McMillan *et al.*, 1994),其谱峰强度相对较弱,在标定全水含量(表示为 C_{H2OT})时由于该峰太弱,导致误差较大,通常不选择该峰(Thomas, 2000; Chabiron *et al.*, 2004; Behrens *et al.*, 2006).

利用共聚焦激光拉曼光谱仪来限定硅酸盐玻璃中的水含量,需要先对标准物质进行谱峰校正,根据标定时选取水的种型和拉曼峰高度/强度的不同,可分为外标和内标两种校正方法(Thomas, 2000).外标法,是一种基于总水含量(C_{H_2OT})与位于高频段(~3 550 cm^{-1}处)总水(H_2O_T)拉曼谱峰的绝对峰高度(I_{H_2O})或强度(A_{H_2O})呈线性关系进行拟合的方法(Stolper, 1982).内标法,是基于玻璃中水含量与相对谱峰高度($I_{H_2O}/I_{T\text{-}O}$)或相对积分强度($A_{H_2O}/A_{T\text{-}O}$)进行拟合的方法,而相对高度或积分强度指的是使用高频段水的伸缩振动拉曼谱峰与低频段 Si(Al)-O 键振动引起的拉曼谱峰的高度或积分强度之比(Matson *et al.*, 1986).

相对于内标法来说,外标法仅仅只考虑~3 550 cm^{-1}处的拉曼峰强度,因此受玻璃成分的影响不大.但近期有研究认为由于溶解在硅酸盐玻璃中水(H_2O_T)的拉曼散射截面与玻璃成分的改变(Behrens *et al.*, 2006; Di Muro *et al.*, 2006a; Mercier *et al.*, 2009),使得利用外标法获得的不同成分的含水硅酸盐玻璃的标定曲线斜率具有较小的误差(Behrens *et al.*, 2006; Di Muro *et al.*, 2006a, 2006b).总体来说,虽然外标法受玻璃成分的影响较小,但是很大程度上却容易受到实验条件和测量条件的人为因素影响,因此为了建立具有更加普适性的标定方法,建议引入对溶解水不敏感的低频段区间的硅氧键振动峰的高度/强度进行内标校正归一化,以减少因为标样成分含量造成的差别,从而获得良好的重现性(Behrens *et al.*, 2006; Di Muro *et al.*, 2006a, 2006b).

3 拉曼光谱仪定量限定硅酸盐玻璃水含量方法的影响因素及校正

影响拉曼光谱定量限定熔体包裹体中水含量的因素,除了受标准样品与待测样品基体匹配外,还受到仪器参数、数据处理等后期影响,包括标样的建立和选择、玻璃/熔体性质和成分、拉曼标定参数的选取、仪器参数选择、拉曼光谱数据处理等.玻璃/熔体成分主要影响拉曼光谱的峰位和峰高;仪器参数的选取则决定了光谱的质量,包括信号强度、重现性、荧光背景等;不同拉曼光谱处理方法以及标定参数的选取也会或多或少影响到不同方法的准确性.

3.1 标准物质的建立和成分的影响

共聚焦激光拉曼光谱仪应用于定量限定熔体包裹体中的水含量时,需要建立一套标准样品用于标定工作曲线,然后对待测样品进行定量标定.因此标样的建立和确定是该实验方法的基础和前提.标样通常为已知且具有不同梯度水含量(0.1%~

16%)的玻璃(数量>6,多多益善),通过拉曼光谱仪测量标样中水的拉曼谱峰的高度/强度与水含量进行线性拟合校正获得水含量标定曲线(Thomas, 2002, 2006; Behrens *et al.*, 2006; Mercier *et al.*, 2009).

标样通常是高温高压活塞圆筒装置合成的具有不同水含量的硅酸盐玻璃,然后通过其他不同的方法(如傅立叶转换红外光谱仪、Karl Fischer滴定法、电子探针等)对其中水的绝对含量进行定量标定.合成含水玻璃标样的初始物质成分包括响岩、安山岩、流纹岩、玄武岩等(Behrens *et al.*, 2006; Schiavi *et al.*, 2018).

含水玻璃的拉曼水峰主要集中在3 550 cm^{-1}附近(Thomas, 2000; Chabiron *et al.*, 2004),前人通过反卷积数学积分变换方法发现该峰可被分解成4个高斯+洛伦兹成分的子峰:3 330,3 458,3 560和3 626 cm^{-1}(Chabiron *et al.*, 2004).其中前两者谱峰(3 330和3 458 cm^{-1})是由分子水H_2O_m的伸缩振动引起,后两者谱峰(3 560和3 626 cm^{-1})归属于羟基水O-H的伸缩振动峰(图2b),不同成分归属的子峰可用于定量限定硅酸盐玻璃中的不同水种型含量分析(Chabiron *et al.*, 2004; Behrens *et al.*, 2006; Di Muro *et al.*, 2006a; Helo *et al.*, 2020).在硅酸盐玻璃中,硅氧四面体中随着桥氧T-O-T(集中在LF区~500 cm^{-1}峰)与非桥氧T-O(集中在HF区~1 000 cm^{-1}峰)的占比变化,与之对应的拉曼主峰也将发生相应的移动(图2a).桥氧键占比越大,其对应的峰高越强,且峰位向低波数偏移(Zajacz *et al.*, 2005; Mercier *et al.*, 2009; Le Losq *et al.*, 2012).此外,研究表明LF_{500}/HF_{1000}拉曼峰高度/强度比值随硅酸盐玻璃中SiO_2含量的升高而升高(Di Muro *et al.*, 2006a, 2006b; Di Genova *et al.*, 2017),对于酸性硅酸盐玻璃(如流纹岩、粗面岩、响岩、英安岩等)具有较强的LF_{500}拉曼峰高度/强度,而对于中性至基性硅酸盐玻璃(如安山岩、玄武岩等)具有较强的HF_{1000}拉曼峰高度/强度(图2a).此外,硅酸盐玻璃中其他元素的加入会激发/增强出其他谱峰,从而显著改变低频区Si(Al)-O的拉曼谱峰位移和其形状(Schiavi *et al.*, 2018).对于安山质和玄武质玻璃,因为Fe元素的增多,使得Fe-O-Si键振动导致940~970 cm^{-1}处会出现拉曼谱峰;而Fe-Ti微晶的形成,会导致670~690 cm^{-1}处出现拉曼谱峰(Sharma *et al.*, 1981; Di Genova *et al.*, 2017; González-García *et al.*, 2021).对于含碳的硅酸盐玻璃,1 062~1 092 cm^{-1}处会出现与碳酸根相关的拉曼峰(Schiavi *et al.*, 2018).因此,不同成分的硅酸盐玻璃会影响拉曼谱峰的位移和强度,特别是对于低频区间硅氧Si(Al)-O键引起的谱峰位移和强度影响最大.因此,为了提高测试的准确度和精度,同时减少由于不同岩性/成分的标样造成的系统偏差,待测样品的岩性/成分需要尽量与硅酸盐玻璃标样相匹配.

3.2　硅酸盐玻璃成分对内标法的影响及标定参数的选取

对于内标法,由于标定参数($I_{H_2O}/I_{T\text{-}O}$或$A_{H_2O}/A_{T\text{-}O}$)中引入了低频段硅氧四面体中Si(Al)-O键的振动峰,而不同成分硅酸盐玻璃在低频段的呈现具有较大差异,因此硅酸盐玻璃的成分对标定结果的影响是显著的.一方面,随着SiO_2含量的增加,LF_{500}主峰变窄,峰高增加峰位向低频数移动,反之,LF_{1000}主峰变宽,峰高降低峰位向高频数移动(Zajacz *et al.*, 2005; Mercier *et al.*, 2009),其结果导致内标法标定不同成分硅酸盐玻璃的曲线斜率具有显著的差别(Zajacz *et al.*, 2005; Behrens *et al.*, 2006);另一方面,次要影响因素有晶格中离子替换,其他成网离子(如Al^{3+},Fe^{3+})或解网离子(Fe^{2+}, Mn^{2+}, Mg^{2+}, Ca^{2+}, Na^{+}, K^{+})含量的不同也会导致拉曼谱峰的变化,尽管这种影响较小,但不可忽略.导致这种变化的主要机理有:(1)硅酸盐骨架中的$(Si^{4+})_{IV}$能被$(Al^{3+})_{IV}$和$(Fe^{3+})_{IV}$替代,$(Al^{3+})_{IV}$的替代会导致~1 030 cm^{-1}处的峰强度降低,~910 cm^{-1}处的峰强度升高,$(Fe^{3+})_{IV}$的替代增加会导致~965 cm^{-1}处的峰强度增加(Di Muro *et al.*, 2006a, 2006b; Mercier *et al.*, 2009; Di Genova *et al.*, 2017);(2)破坏桥氧T-O-T连接的碱土金属氧化物的引入会导致非桥氧的增加(Di Muro *et al.*, 2006a),水含量的变化引起的玻璃聚合度发生变化,而使~1 060 cm^{-1}的峰发生变化,从而影响标定方法的准确性(Mercier *et al.*, 2009; Di Genova *et al.*, 2017).

由于硅酸盐玻璃成分的差异造成低频段主峰位置和高度/强度值的不同,从而影响标定参数($I_{H_2O}/I_{T\text{-}O}$或$A_{H_2O}/A_{T\text{-}O}$).因此,在使用内标法时,标定参数的选择需要考虑硅酸盐玻璃成分.对于酸性硅酸盐玻璃(初始物质如流纹岩、粗面岩、响岩、英安

岩等),选择使用LF_{500}峰段进行校正,即I_{H_2O}/I_{LF}或A_{H_2O}/A_{LF}作为最佳的标定参数;对于中性至基性硅酸盐玻璃(如安山岩、玄武岩等),选择使用HF_{1000}峰段进行校正,即I_{H_2O}/I_{HF}或A_{H_2O}/A_{HF}为最佳标定参数(Behrens *et al.*, 2006; Mercier *et al.*, 2009; Bonechi *et al.*, 2022).Behrens *et al.*(2006)在使用A_{H_2O}/A_{HF+LF}作为标定参数时,标定结果存在一定的误差(Behrens *et al.*, 2006),这可能与基线处理方式、Fe^{3+}的影响有关,当考虑到这些因素时,A_{H_2O}/A_{HF+LF}也可作为不同成分硅酸盐玻璃的标定参数(Le Losq *et al.*, 2012; Di Genova *et al.*, 2017; Schiavi *et al.*, 2018).考虑到成分复杂性,有学者尝试建立与成分无关的标定方法.Zajacz *et al.*(2005)提出引入两个参数:应用数学积分变换方法对HF_{1000}峰进行分解,同时需要考虑$(Al^{3+})_{IV}$和$(Fe^{3+})_{IV}$替代$(Si^{4+})_{IV}$的影响,在此基础上拟合了经验校正公式(1)(Zajacz *et al.*, 2005).Mercier *et al.*(2010)对玻璃聚合度、总水含量、铁离子的氧化状态等因素进行函数化,推导出适用于未知成分的硅酸盐玻璃的水含量计算公式(2)(Mercier *et al.*, 2009, 2010),通过调整各项结构参数即可估算硅酸盐玻璃中水含量.Le Losq *et al.*(2012)用特殊的基线处理方法,选取总水峰与整个低频区的拉曼峰的相对强度比值(A_{H_2OT}/A_{T-O})为标定参数进行拟合,从而得出一个适用于各种成分玻璃中总水含量的标定公式(3)(Le Losq *et al.*, 2012).

$$C_{H_2O}(\%)=0.211\frac{A_{H_2OT}}{A_{T-O}}\times\left[\frac{1\,130-P_{T-O}}{95}+0.69\right]T_{tot}, \tag{1}$$

$$C_{H_2O}(\%)=\frac{\left[\left(f\left(\frac{NBO}{T};SM\right)\times I^{samp}_{H_2OT}/\left(I^{samp}_{LF}/I^{samp}_{HF}\right)\right)-q\right]}{k}, \tag{2}$$

$$C_{H_2O}(\%)=100\cdot\alpha\cdot(A_{H_2OT}/A_{T-O})/[1+\alpha\cdot(A_{H_2OT}/A_{T-O})], \tag{3}$$

公式(1)中,A_{H_2OT}代表总水峰的积分强度,A_{T-O}代表850~1 250 cm^{-1}峰段的积分强度,P_{T-O}代表HF_{1000}内最强峰的峰位,T_{tot}代表四面体阳离子的总数(由电子探针数据可获得);公式(2)中,f(NBO/T;SM)代表与每个四面体配位离子结合的非桥氧数量和解网离子数量有关的函数,$I^{samp}_{H_2OT}$、I^{samp}_{LF}、I^{samp}_{HF}分别代表待测样品在总水峰、LF_{500}、HF_{1000}处的峰高度,k是与光学系统相关的参数,q是聚焦的系统误差;公式(3)中,A_{H_2O}和A_{T-O}分别代表待测样品在水峰和在硅酸盐中硅氧键振动全谱峰的积分强度,标定直线斜率$\alpha=0.007\,609$.

总的来说虽然内标法受到玻璃标样自身成分的影响,但这种影响可以通过选取合适的标定参数和公式进行消除,因此,内标法依然是标定含水硅酸盐玻璃中水含量的准确且可靠的方法.

3.3 待测样品的聚焦深度

由于熔体包裹体内通常富含大量的液态或气态挥发分而极不稳定,特别是当把包裹体抛光暴露于表面时,很可能导致其内的挥发分丢失,特别是水含量发生丢失.而共聚焦激光拉曼光谱仪不仅可以分析暴露于表面的样品,而且可以通过针孔共聚焦分析位于样品表面以下的区间,因此是研究熔体包裹体的理想手段.在使用拉曼光谱仪测定分析未暴露在表面的包裹体时,聚焦样品的深度显得较为重要,它影响拉曼峰高度/强度,从而影响水含量的测定(Chabiron *et al.*, 2004; Thomas *et al.*, 2006).Thomas *et al.*(2006)通过选取世界上不同地区的3件样品(包括德国Zinnwald地区E-Erzgebirge富钠长石花岗岩内石英中熔体包裹体、德国Ehrenfriedersdorf地区和Central-Erzgebirge地区伟晶岩石英中熔体包裹体、意大利Etna地区火山橄榄石晶体中的熔体包裹体),利用拉曼光谱仪对熔体包裹体纵向聚焦深度研究时发现,聚焦深度与测量的水含量之间有明显的负相关,即聚焦深度越深其测量的水含量越小.Behrens *et al.*(2006)在对均一的玻璃标样进行水含量校正时也发现了同一现象,并认为当激光聚焦面处于样品表面以下10±5 μm深度时,拉曼峰的信号强度值最大,在大于15 μm以下的深度,信号强度明显下降(Behrens *et al.*,2006; Mercier *et al.*, 2009; Schiavi *et al.*, 2018).信号强度随激光聚焦深度变化的根本原因不仅在于含水玻璃或熔体包裹体的寄主矿物对激光信号具有一定的吸收能力,且不同成分的玻璃或不同寄主矿物的吸光系数不一样,导致信号衰减程度也不一样.综合以上实验结果来看,位于样品表面以下约10±5 μm处的聚焦深度较为理想,不仅能够获得最大强度的拉曼光谱峰值,而且测量范围处于待测样品信号采集的最佳位置,能够保持较好的信噪比.

3.4　激光拉曼光谱仪参数的设置

拉曼光谱的数字定量化标定是影响水含量的直接因素,无论是内标法还是外标法,都需要准确获得具有谱峰强度高、重现性好、荧光背景低等特点的最佳拉曼光谱数据.特别是外标法,仅仅选取~3 550 cm^{-1}全水峰(I_{H_2OT}或A_{H_2OT})作为标定参数,它强烈依赖于拉曼光谱仪各项参数的设置,包括激光光源、激光能量、采集时间及次数、光栅、共聚焦程度、物镜大小,因此测试时最佳参数的设置是至关重要的.

对于拉曼光谱仪的激光器选择,大部分研究者均选用绿光光源 532 和 514 nm,以及蓝光光源 488 nm 激光器,此差异由不同型号的拉曼光谱仪配备不同波长的激光导致.Severs *et al.*(2007)认为 244 nm 的紫外光光源可使激光激发的荧光干扰最小化,但目前为止大部分的研究者仍然采用 532 nm 的激光器,认为绝大部分的样品不受荧光的干扰,即使有荧光效应的产生也可以在后期处理时进行消除(Zajacz *et al.*, 2005; Di Muro *et al.*, 2006a, 2006b; Le Losq *et al.*, 2012).Behrens *et al.*(2006)在使用外标法标定中发现测量时选择不同物镜可导致结果出现一定的差异,认为采用 100× 物镜镜头结合小的共焦孔径,可降低采样深度的同时增大采样体积,增强拉曼信号强度(Di Muro *et al.*, 2006a, 2006b).采用不同大小的光栅获得的光谱各有优点,在使用光栅时,光栅刻线越密(1 800/2 400 grooves/mm),其光谱分辨率越高,信号衰减越强,分析时间也较长,同时需要多个窗口进行采集(Thomas, 2000; Zajacz *et al.*, 2005; Behrens *et al.*, 2006; Thomas *et al.*, 2006; Severs *et al.*, 2007),而低密度光栅(如 600 grooves/mm)虽然光谱分辨率较低,信号衰减较少,但是可快速获得 800~4 000 cm^{-1}频率范围内的拉曼光谱(Chabiron *et al.*, 2004; Di Muro *et al.*, 2006a, 2006b; Behrens *et al.*, 2006; Mercier *et al.*, 2009).

为了保证获得强度高且重复性好的光谱,较短收集时间和较低激光能量(指作用于样品表面的激光能量)通常被用于收集硅酸盐玻璃标样的拉曼光谱.当硅酸盐玻璃标样受长时间或高能量激光照射时,通常长时间的局部受热会导致玻璃氧化甚至熔融,从而导致水的丢失.而对于含 Fe 硅酸盐玻璃,其内部含有铁氧化物微晶时,在受到长时间激光照射时,其内部的铁氧化物微晶(赤铁矿)会氧化成磁赤铁矿,而导致磁赤铁矿内 300~800 cm^{-1}间的拉曼峰与玻璃标样中 Si(Al)-O 键的拉曼峰发生重合,从而影响标定参数的准确性(Liebske *et al.*, 2003; Di Muro *et al.*, 2006a, 2006b; Behrens *et al.*, 2006; Mercier *et al.*, 2009).因此,大部分研究者认为,采用较短收集时间和较低激光能量来分析硅酸盐玻璃样品是必要的,合适的激光能量(样品表面)为 7~11 mW 之间.对不同水含量的硅酸盐玻璃样品采用的收集时间和次数也不尽相同,通常低水含量的样品需要更长的收集时间以提高信噪比.然而,Le Losq *et al.*(2012)尝试在铁含量高的样品中,使用了较大的激光能量和较长的采集时间作用于样品表面,并未发现激光对样品有所破坏,认为实际的采集时间及激光能量对样品的破坏并不能一概而论,而要视实际而定.无论如何,这些参数的调整其最终目的都是获得强度高、重现性好、高质量的拉曼光谱信号.

3.5　激光拉曼图谱数据处理

由于硅酸盐玻璃的拉曼光谱受成分、仪器及测试环境影响,因此需扣除拉曼光谱基线,然后对所得光谱进行再次校准,是准确获得标定方法的重要步骤.拉曼散射效率是随拉曼频移锐减的函数,其绝对强度受到温度和频率的影响,因此需要引入 Long(1977)建立的公式,用温度和频率两个参数的拉曼光谱进行校正;为消除仪器引起的噪声,优化荧光和峰重叠效应,通常采用直线基线、三次样条插值或二阶多项式等方法进行基线扣除,目前,最常用的基线处理方法是同时结合 Long(1977)校正和三次样条插值的使用(Zajacz *et al.*, 2005; Behrens *et al.*, 2006; Severs *et al.*, 2007; Le Losq *et al.*, 2012; Di Genova *et al.*, 2017; Schiavi *et al.*, 2018).Le Losq *et al.*(2012)进一步根据硅酸盐中 SiO_2的含量提出分段式固定部分基线,然后再使用三次样条插值法进行基线的整体扣除,从而消除硅酸盐玻璃成分、荧光和重叠峰的影响,此方法也得到了后期研究的检验和应用(Di Genova *et al.*, 2017; Schiavi *et al.*, 2018).

尽管共聚焦激光拉曼光谱仪定量测水的方法在天然的地质样品研究中还存在一些局限,但是通过目前对于拉曼光谱技术方面的开发和理论的认知,不论是硅酸盐玻璃标样的建立,玻璃/熔体性质和成分、拉曼标定参数的选取、仪器参数选择、拉曼光谱数据处理等影响因素,都有较好的校正方法和

公式,这些公式可被用于提高测试的准确度和精度,因此基于激光拉曼光谱仪建立的内标法和外标法是理想的原位无损快速的测量熔体包裹体中水含量的方法,可以被广泛应用于示踪不同研究体系中的熔体、岩浆中的水含量和种型(McMillan and Hofmeister, 1988; Ihinger *et al.*, 1994; Chabiron *et al.*, 1999; Thomas, 2000, 2002; Zajacz *et al.*, 2005; Di Muro *et al.*, 2006a, 2006b; Thomas *et al.*, 2006, 2008; Mercier *et al.*, 2009; Bartoli *et al.*, 2013a; Ferrero *et al.*, 2015, 2016; Schiavi *et al.*, 2018; González-García *et al.*, 2020).

4 激光拉曼光谱仪定量测定熔体包裹体中水含量的地质应用

大陆碰撞过程中会发生广泛的部分熔融现象,形成深熔熔体.深入认识深熔熔体的形成和演化是大陆俯冲带化学地球动力学的主要研究内容(Labrousse *et al.*, 2002; Wallis *et al.*, 2005; Zheng *et al.*, 2011).深熔熔体极不稳定且容易受到后期地质作用的影响,而现有技术很难在如此深的地幔/地壳条件下直接测定其熔体相(Zhang *et al.*, 2008; Zheng *et al.*, 2011).但深熔熔体却可以被高压/超高压变质地体中的转熔矿物所捕获并形成熔体包裹体.捕获后的熔体常常受到熔体成分、变质演化过程轨迹及包裹体粒径等影响(Frezzotti, 2001; Wallace, 2005; Holness *et al.*, 2011),小颗粒熔体在快速冷却时易形成均一的玻璃质,而缓慢冷却时熔体则会结晶出长石、石英等多相晶体包裹体(固体相±流体相)(Gao *et al.*, 2017; 王蝶等, 2017).由于被转熔矿物(如石榴子石、绿辉石、锆石等)紧密包裹的熔体包裹体,一般不容易受到外部条件及后期过程的改造,因此是探究深俯冲大陆地壳深熔的最直接也是最理想的研究对象(Zeng *et al.*, 2009; Gao *et al.*, 2012, 2013, 2017; Hermann *et al.*, 2013; Liu *et al.*, 2013, 2020).

4.1 在岩浆岩中的应用

在岩浆侵入岩和喷出岩中,早期结晶的矿物可以捕获共存的熔体并形成均一相的玻璃质熔体包裹体,因此被率先用于激光拉曼光谱仪定量限定岩浆熔体中的水含量和水种型(Thomas, 2000; Chabiron *et al.*, 2004; Di Muro *et al.*, 2006a, 2006b; Müller *et al.*, 2006a; Thomas *et al.*, 2006; González-García *et al.*, 2020; Venugopal *et al.*, 2020; Bonechi *et al.*, 2022).前人对花岗岩和玄武岩矿物中的熔体包裹体进行了标定,认为拉曼光谱可定量分析较小尺寸的熔体包裹体(直径>3 μm)中高达39%的水含量,精度可达±0.15%(Thomas, 2000, 2002; Müller *et al.*, 2006b),并且建立了对包裹于矿物内部并未暴露表面的同源熔体包裹体中水含量的测试方法(Thomas *et al.*, 2006),此方法的建立在避免激光加热造成熔体包裹体水的丢失的同时,也给天然样品的制样提供了极大的便利.

因此,近十几年,利用激光拉曼光谱仪测试熔体包裹体中水含量的方法被广泛用于岩浆岩研究领域,其测试对象主要包括侵入岩或喷出岩中的大颗粒矿物斑晶(如石英斑晶,Chabiron *et al.*, 2004; Zajacz *et al.*, 2005; Müller *et al.*, 2006a,2006b; Kotov *et al.*, 2017; 长石斑晶,Kotov *et al.*, 2017; 橄榄石斑晶,Mercier *et al.*, 2010)内的熔体包裹体和岩浆喷出的产物(如浮岩,Le Losq *et al.*, 2012; 黑曜岩,Angelopoulos *et al.*, 2020).对不均一的火山浮岩进行剖面水含量的精确分析,结果表明熔体水含量影响其流变学性质,从而导致富水熔体和贫水熔体由于明显的密度和流变学性质差异形成界面张力梯度,最终影响岩浆流动和分离前瞬时的流变学行为(Le Losq *et al.*, 2012).此外,Kotov *et al.*(2017)通过建立斜长石的An环带与其内熔体包裹体水含量之间的关系,发现当岩浆中的水含量达到过饱和,水分压增大,可导致岩浆发生脱气作用,斜长石An值增大,脱气作用完成后水分压降低而重新达到平衡,在灾难性火山爆发之前,岩浆中的水含量可能再次达到饱和(Kotov *et al.*, 2017),这一研究同时也印证了岩浆演化过程中水含量的不断变化,同一地区的喷出岩和侵入岩中熔体包裹体水含量变化相当大,揭示了它们来源于不同层位的岩浆房(Müller *et al.*, 2006a).

4.2 在变质岩中的应用

近年来高压-超高压岩石的部分熔融在世界范围内很多碰撞造山带中逐渐被认识并得到深入研究(Labrousse *et al.*, 2011; Zheng *et al.*, 2011; Stepanov *et al.*, 2014; Zheng and Hermann, 2014).作为代表初始熔体的多相晶体包裹体也先后在许多的高压-超高压地体中被发现,如中国大别-苏鲁变质带(Enami and Zang, 1990; Enami *et al.*,

1993; Yang *et al.*, 1998; Zeng *et al.*, 2009, 2013; Gao *et al.*, 2012, 2013)、德国 Erzgebirge 地体(Hwang *et al.*, 2001; Massonne, 2001; Massonne and Nasdala, 2003)、哈萨克斯坦 Kokchetav 地体(Mikhno and Korsakov, 2013; Mikhno *et al.*, 2013; Stepanov *et al.*, 2016)和中国西部的北柴达木地体(Song *et al.*, 2003; Zhang *et al.*, 2009).尽管这种多晶包裹体组分具有高度不均一性,仍然有学者尝试通过均一化实验,并成功使其重熔为均质玻璃,以便进行微区原位主微量成分和水含量的分析(Korsakov and Hermann, 2006; Malaspina *et al.*, 2006; Cesare *et al.*, 2009, 2011; Bartoli *et al.*, 2013a; Ferrero *et al.*, 2015; Stepanov *et al.*, 2016; Bodnar and Frezzotti, 2020).尽管前人通过实验岩石学研究发现,经历持续较长时间的加热(>1 512 h)可以导致75%的熔体包裹体中的水含量逃逸,但是认为不超过12 h的均一化加热过程对熔体包裹体中水的逃逸和扩散影响微乎其微(Severs *et al.*, 2007),国际著名的熔体包裹体意大利研究小组, Bartoli *et al.*(2013a)和 Ferrero *et al.*(2015)首次尝试利用共聚焦激光拉曼光谱仪测试了均一化后的多晶包裹体中的水含量,并分别尝试使用外标(Bartoli *et al.*, 2013a)和内标(Ferrero *et al.*, 2015)校正法,成功获得了熔体包裹体中水含量,结合其结构和主量元素特征,进一步模拟了俯冲带内地幔深度熔融过程的条件和熔体产生的量,揭示了除降压熔融外,在变质峰期条件下也可以发生部分熔融产生高压熔体,认为即使少量熔体的产生也可以显著提升并改变岩石流变学性质从而促使超高压岩石发生折返(Bartoli *et al.*, 2013a, 2015; Cesare *et al.*, 2015; Ferrero *et al.*, 2015).此外,根据均一化后熔体包裹体的水含量和主要成分计算的粘度比常见的花岗质熔体粘度大2~3个数量级,这表明深熔熔体在分离和上升过程上有更低的速率和更长的时限(Bartoli *et al.*, 2013a).但是近期的研究发现,对于富含大量挥发分气泡的熔体包裹体在均一化过程中,气泡可以隔离部分主量元素和挥发分元素,使测量值低于原始初始熔体的水含量(Venugopal *et al.*, 2020).

这些研究虽然都处于起步和摸索阶段,但是都显示出共聚焦激光拉曼光谱仪定量限定水含量的方法具有高的空间分辨率、高灵敏度、无损、快速、高效、制样简单等优点,且可以同时分析暴露于表面或包裹于内部的样品,因此具有较大的应用范围和应用前景,该方法不仅可以定量限定岩浆及深熔熔体中水含量和水种型,而且对于模拟地壳深俯冲和初始折返过程及深熔熔体的分离和上升过程具有广阔的前景,为探究地壳深熔机制、熔体演化规律以及陆壳分异等过程提供重要的信息(Zheng, 2012; Bartoli *et al.*, 2013a, 2013b, 2015; Ferrero *et al.*, 2015).

致谢:感谢两位匿名审稿人对本文提出的建设性修改意见.本研究获得中国国家自然科学基金委(42072070)和中央高校基本科研业务费专项资金资助(WK2080000128)的资助.

References

Angelopoulos, P.M., Manić, N., Tsakiridis, P., et al., 2020. Dehydration of Rhyolite: Activation Energy, Water Speciation and Morphological Investigation. *Journal of Thermal Analysis and Calorimetry*, 142(1): 395−407. https://doi.org/10.1007/s10973-020-10105-2

Bartoli, O., Acosta-Vigil, A., Cesare, B., 2015. High-Temperature Metamorphism and Crustal Melting: Working with Melt Inclusions. *Periodico di Mineralogia*, 84(3B): 591−614. https://doi. org/10.2451/2015PM0434

Bartoli, O., Acosta-Vigil, A., Ferrero, S., et al., 2016. Granitoid Magmas Preserved as Melt Inclusions in High-Grade Metamorphic Rock. *American Mineralogist*, 101(7): 1543−1559. https://doi. org/10.2138/am-2016-5541ccbyncnd

Bartoli, O., Cesare, B., Poli, S., et al., 2013a. Nanogranite Inclusions in Migmatitic Garnet: Behavior during Piston-Cylinder Remelting Experiments. *Geofluids*, 13(4): 405−420. https://doi.org/10.1111/gfl.12038

Bartoli, O., Cesare, B., Poli, S., et al., 2013b. Recovering the Composition of Melt and the Fluid Regime at the Onset of Crustal Anatexis and S-Type Granite Formation. *Geology*, 41(2): 115−118. https://doi. org/10.1130/g33455.1

Beaumont, C., Jamieson, R., Nguyen, M, 2010. Models of Large, Hot Orogens Containing a Collage of Reworked and Accreted Terranes. *Canadian Journal of Earth Sciences*, 47(4): 485−515. https://doi. org/10.1139/E10-002

Behrens, H., Roux, J., Neuville, D.R., et al., 2006. Quantification of Dissolved H_2O in Silicate Glasses Using Confocal microRaman Spectroscopy. *Chemical Geology*, 229(1/2/3): 96−112. https://doi. org/10.1016/j. chem-

geo.2006.01.014

Berndt, J., Koepke, J., Holtz, F., 2005. An Experimental Investigation of the Influence of Water and Oxygen Fugacity on Differentiation of MORB at 200 MPa. *Journal of Petrology*, 46(1): 135－167. https://doi. org/10.1093/petrology/egh066

Bodnar, R. J., Frezzotti, M. L., 2020. Microscale Chemistry: Raman Analysis of Fluid and Melt Inclusions. *Elements*, 16 (2): 93－98. https://doi.org/10.2138/gselements.16.2.93

Bonechi, B., Gaeta, M., Perinelli, C., et al., 2022. Micro-Raman Water Calibration in Ultrapotassic Silicate Glasses: Application to Phono-Tephrites and K-Foidites of Colli Albani Volcanic District (Central Italy). *Chemical Geology*, 597: 120816. https://doi.org/10.1016/j.chemgeo.2022.120816

Brown, M., 2013. Granite: From Genesis to Emplacement. *Geological Society of America Bulletin*, 125(7－8): 1079－1113. https://doi.org/10.1130/b30877.1

Brown, M., Rushmer, T., 2006. Evolution and Differentiation of the Continental Crust. Cambridge University Press, Cambridge.

Cesare, B., Acosta-Vigil, A., Bartoli, O., et al., 2015. What can we Learn from Melt Inclusions in Migmatites and Granulites? *Lithos*, 239: 186－216. https://doi. org/10.1016/j.lithos.2015.09.028

Cesare, B., Acosta-Vigil, A., Ferrero, S., et al., 2011. Melt Inclusions in Migmatites and Granulites. *Journal of the Virtual Explorer*, 38. https://doi. org/10.3809/jvirtex.2011.00268

Cesare, B., Ferrero, S., Salvioli-Mariani, E., et al., 2009. "Nanogranite" and Glassy Inclusions: The Anatectic Melt in Migmatites and Granulites. *Geology*, 37(7): 627－630. https://doi.org/10.1130/g25759a.1

Chabiron, A., Peiffert, C., Pironon, J., et al., 1999. Determination of Water Content in Melt Inclusions by Raman Spectrometry. In: Ristedt, H., Luders, V., Thomas, R., eds., ECROFI XV (European Current Research on Fluid Inclusions), Abstract Program. *Terra Nostra-Schr Alfred-Wegner-Stiftung*, 99(6): 68－69.

Chabiron, A., Pironon, J., Massare, D., 2004. Characterization of Water in Synthetic Rhyolitic Glasses and Natural Melt Inclusions by Raman Spectroscopy. *Contributions to Mineralogy and Petrology*, 146(4): 485－492. https://doi.org/10.1007/s00410-003-0510-x

Chen, R.X., Zheng, Y.F., Gong, B., 2011. Mineral Hydrogen Isotopes and Water Contents in Ultrahigh-Pressure Metabasite and Metagranite: Constraints on Fluid Flow during Continental Subduction-Zone Metamorphism. *Chemical Geology*, 281(1/2): 103－124. https://doi. org/10.1016/j.chemgeo.2010.12.002

Chen, R. X., Zheng, Y. F., Gong, B., 2007. Fluid Activity in Continental Subduction Zones: Insights from Stable Isotopes and Water Contents in Minerals from Ultrahigh-Pressure Metamorphic Rocks. *Acta Petrologica Sinica*, 27: 451－468.

Chen, Y.X., Zheng, Y.F., Gao, X.Y., et al., 2014. Multiphase Solid Inclusions in Zoisite-Bearing Eclogite: Evidence for Partial Melting of Ultrahigh-Pressure Metamorphic Rocks during Continental Collision. *Lithos*, 200/201: 1－21. https://doi.org/10.1016/j.lithos.2014.04.004

Darling, R.S., 2013. Zircon-Bearing, Crystallized Melt Inclusions in Peritectic Garnet from the Western Adirondack Mountains, New York State, USA. *Geofluids*, 13(4): 453－459. https://doi.org/10.1111/gfl.12047

Deloule, É., Paillat, O., Pichavant, M., et al., 1995. Ion Microprobe Determination of Water in Silicate Glasses: Methods and Applications. *Chemical Geology*, 125(1－2): 19－28. https://doi.org/10.1016/0009-2541(95)00070-3

Devine, J.D., Gardner, J.E., Brack, H.P., et al., 1995. Comparison of Microanalytical Methods for Estimating H_2O Contents of Silicic Volcanic Glasses. *American Mineralogist*, 80(3/4): 319－328. https://doi.org/10.2138/am-1995-3-413

Di Genova, D., Sicola, S., Romano, C., et al., 2017. Effect of Iron and Nanolites on Raman Spectra of Volcanic Glasses: A Reassessment of Existing Strategies to Estimate the Water Content. *Chemical Geology*, 475: 76－86. https://doi.org/10.1016/j.chemgeo.2017.10.035

Di Muro, A., Villemant, B., Montagnac, G., et al., 2006a. Quantification of Water Content and Speciation in Natural Silicic Glasses (Phonolite, Dacite, Rhyolite) by Confocal microRaman Spectrometry. *Geochimica et Cosmochimica Acta*, 70(11): 2868－2884. https://doi. org/10.1016/j.gca.2006.02.016

Di Muro, A., Giordano, D., Villemant, B., et al., 2006b. Influence of Composition and Thermal History of Volcanic Glasses on Water Content as Determined by Micro-Raman Spectrometry. *Applied Geochemistry*, 21(5): 802－812. https://doi.org/10.1016/j.apgeochem.2006.02.009

Enami, M., Zang, Q. J., 1990. Quartz Pseudomorphs after Coesite in Eclogites from Shandong Province, East China. *American Mineralogist,* 75(3－4): 381－386.

Enami, M., Zang, Q.J., Yin, Y.J., 1993. High-Pressure Eclogites in Northern Jiangsu-Southern Shandong Province, Eastern China. *Journal of Metamorphic Geology*, 11(4): 589－603.

Ferrero, S., Bartoli, O., Cesare, B., et al., 2012. Microstructures of Melt Inclusions in Anatectic Metasedimentary Rocks. *Journal of Metamorphic Geology*, 30(3): 303－322. https://doi.org/10.1111/j.1525-1314.2011.00968.x

Ferrero, S., Braga, R., Berkesi, M., et al., 2014. Production of Metaluminous Melt during Fluid-Present Anatexis: an Example from the Maghrebian Basement, La Galite Archipelago, Central Mediterranean. *Journal of Metamorphic Geology*, 32(2): 209－225. https://doi.org/10.1111/jmg.12068

Ferrero, S., Godard, G., Palmeri, R., et al., 2018. Partial Melting of Ultramafic Granulites from Dronning Maud Land, Antarctica: Constraints from Melt Inclusions and Thermodynamic Modeling. *American Mineralogist*, 103(4): 610－622. https://doi.org/10.2138/am-2018-6214

Ferrero, S., Wunder, B., Walczak, K., et al., 2015. Preserved near Ultrahigh-Pressure Melt from Continental Crust Subducted to Mantle Depths. *Geology*, 43(5): 447－450. https://doi.org/10.1130/g36534.1

Ferrero, S., Wunder, B., Ziemann, M.A., et al., 2016. Carbonatitic and Granitic Melts Produced under Conditions of Primary Immiscibility during Anatexis in the Lower Crust. *Earth and Planetary Science Letters*, 454: 121－131. https://doi.org/10.1016/j.epsl.2016.08.043

Frezzotti, M. L., 2001. Silicate-Melt Inclusions in Magmatic Rocks: Applications to Petrology. *Lithos*, 55(1－4): 273－299. https://doi. org/10.1016/S0024-4937(00)00048-7

Gao, X.Y., 2019. Large-Scale Flow of Metamorphic Fluids in a Continental Subduction Zone: Evidence from Coesite-Bearing Jadeite Quartzite in the Dabie Orogen. *Earth Science*, 44(12): 4064－4071(in Chinese with English abstract).

Gao, X.Y., Chen, Y.X., Zhang, Q.Q., 2017. Multiphase Solid Inclusions in Ultrahigh-Pressure Metamorphic Rocks: A Snapshot of Anatectic Melts during Continental Collision. *Journal of Asian Earth Sciences*, 145: 192－204. https://doi.org/10.1016/j.jseaes.2017.03.036

Gao, X.Y., Zheng, Y.F., Chen, Y.X., 2012. Dehydration Melting of Ultrahigh-Pressure Eclogite in the Dabie Orogen: Evidence from Multiphase Solid Inclusions in Garnet. *Journal of Metamorphic Geology*, 30(2): 193－212. https://doi.org/10.1111/j.1525-1314.2011.00962.x

Gao, X.Y., Zheng, Y.F., Chen, Y.X., et al., 2013. Trace Element Composition of Continentally Subducted Slab-Derived Melt: Insight from Multiphase Solid Inclusions in Ultrahigh-Pressure Eclogite in the Dabie Orogen. *Journal of Metamorphic Geology*, 31: 453－468. https://doi.org/10.1111/jmg.12029

Gao, X.Y., Zheng, Y.F., Chen, Y.X., et al., 2014. Composite Carbonate and Silicate Multiphase Solid Inclusions in Metamorphic Garnet from Ultrahigh-P Eclogite in the Dabie Orogen. *Journal of Metamorphic Geology*, 32: 961－980. https://doi.org/10.1111/jmg.12102

Giordano, D., Potuzak, M., Romano, C., et al., 2008. Viscosity and Glass Transition Temperature of Hydrous Melts in the System $CaAl_2Si_2O_8$-$CaMgSi_2O_6$. *Chemical Geology*, 256(3/4): 203－215. https://doi.org/10.1016/j.chemgeo.2008.06.027

Gong, B., Chen, R.X., Zheng, Y.F., 2013. Water Contents and Hydrogen Isotopes in Nominally Anhydrous Minerals from UHP Metamorphic Rocks in the Dabie-Sulu Orogenic Belt. *Chinese Science Bulletin*, 58(35): 4384－4389. https://doi.org/10.1007/s11434-013-6069-7

González-García, D., Petrelli, M., Behrens, H., et al., 2018. Diffusive Exchange of Trace Elements between Alkaline Melts: Implications for Element Fractionation and Timescale Estimations during Magma Mixing. *Geochimica et Cosmochimica Acta*, 233: 95－114. https://doi.org/10.1016/j.gca.2018.05.003

González-García, D., Giordano, D., Allabar, A., et al., 2021. Retrieving Dissolved H_2O Content from Micro-Raman Spectroscopy on Nanolitized Silicic Glasses: Application to Volcanic Products of the Paraná Magmatic Province, Brazil. *Chemical Geology*, 567: 120058. https://doi.org/10.1016/j.chemgeo.2021.120058

González-García, D., Giordano, D., Russell, J.K., et al., 2020. A Raman Spectroscopic Tool to Estimate Chemical Composition of Natural Volcanic Glasses. *Chemical Geology*, 556: 119819. https://doi. org/10.1016/j. chemgeo.2020.119819

González-García, D., Vetere, F., Behrens, H., et al., 2019. Interdiffusion of Major Elements at 1 Atmosphere between Natural Shoshonitic and Rhyolitic Melts. *American Mineralogist*, 104(10): 1444－1454. https://doi. org/10.2138/am-2019-6997

Groppo, C., Rolfo, F., Indares, A., 2012. Partial Melting in the Higher Himalayan Crystallines of Eastern Nepal: The Effect of Decompression and Implications for the 'Channel Flow' Model. *Journal of Petrology*, 53(5): 1057－1088. https://doi.org/10.1093/petrology/egs009

Grove, T.L., Till, C.B., Krawczynski, M.J., 2012. The Role of H_2O in Subduction Zone Magmatism. *Annual Review of Earth and Planetary Sciences*, 40: 413－439. https://doi.org/10.1146/annurev-earth-042711-105310

Hacker, B. R., Peacock, S. M., Abers, G. A., et al., 2003.

Subduction Factory 2. are Intermediate-Depth Earthquakes in Subducting Slabs Linked to Metamorphic Dehydration Reactions? *Journal of Geophysical Research: Solid Earth*, 108(B1): 2030. https://doi.org/10.1029/2001jb001129

Halter, W.E., Pettke, T., Heinrich, C.A., et al., 2002. Major to Trace Element Analysis of Melt Inclusions by Laser-Ablation ICP-MS: Methods of Quantification. *Chemical Geology*, 183(1—4): 63—86. https://doi.org/10.1016/S0009-2541(01)00372-2

Hauri, E., Wang, J.H., Dixon, J.E., et al., 2002. SIMS Analysis of Volatiles in Silicate Glasses. *Chemical Geology*, 183(1—4): 99—114. https://doi.org/10.1016/S0009-2541(01)00375-8

Helo, C., Castro, J.M., Hess, K.U., et al., 2020. Determination of Water Speciation in Hydrous Haplogranitic Glasses with Partial Raman Spectra. *Chemical Geology*, 553: 119793. https://doi.org/10.1016/j.chemgeo.2020.119793

Hermann, J., Zheng, Y.F., Rubatto, D., 2013. Deep Fluids in Subducted Continental Crust. *Elements*, 9(4): 281—287. https://doi.org/10.2113/gselements.9.4.281

Hier—Majumder, S., Anderson, I.M., Kohlstedt, D.L., 1997. Influence of Protons on Fe-Mg Interdiffusion in High-Magnesian Andesitic Melts. *Geology*, 25: 42—44.

Hirth, G., Kohlstedt, D., 2003. Rheology of the Upper Mantle and the Mantle Wedge: A View from the Experimentalists. Inside the Subduction Factory. Washington, D. C.: American Geophysical Union, 83—105. https://doi.org/10.1029/138gm06

Hofmeister, A.M., 2004. Enhancement of Radiative Transfer in the Upper Mantle by OH^- in Minerals. *Physics of the Earth and Planetary Interiors*, 146(3/4): 483—495. https://doi.org/10.1016/j.pepi.2004.05.007

Holness, M. B., Cesare, B., Sawyer, E. W., 2011. Melted Rocks under the Microscope: Microstructures and Their Interpretation. *Elements*, 7(4): 247—252. https://doi.org/10.2113/gselements.7.4.247

Hui, H.J., Zhang, Y.X., 2007. Toward a General Viscosity Equation for Natural Anhydrous and Hydrous Silicate Melts. *Geochimica et Cosmochimica Acta*, 71(2): 403—416. https://doi.org/10.1016/j.gca.2006.09.003

Hwang, S.L., Shen, P.Y., Chu, H.T., et al., 2001. Genesis of Microdiamonds from Melt and Associated Multiphase Inclusions in Garnet of Ultrahigh-Pressure Gneiss from Erzgebirge, Germany. *Earth and Planetary Science Letters*, 188(1/2): 9—15. https://doi.org/10.1016/S0012-821X(01)00314-4

Ihinger, P.D., Hervig, R.L., McMillan, P.F., 1994. Analytical Methods Forvolatiles in Glasses. In: Carroll, M.-R., Holloway, J.R., eds., Volatiles in Magmas 30. Reviews in Mineralogy, Mineralogical Society of America, Chantilly, Virginia.

Karato, S., 1990. The Role of Hydrogen in the Electrical Conductivity of the Upper Mantle. *Nature*, 347(6290): 272—273. https://doi.org/10.1038/347272a0

Karato, S.I., 2010. Rheology of the Deep Upper Mantle and Its Implications for the Preservation of the Continental Roots: A Review. *Tectonophysics*, 481(1/2/3/4): 82—98. https://doi.org/10.1016/j.tecto.2009.04.011

Kelley, K.A., Plank, T., Newman, S., et al., 2010. Mantle Melting as a Function of Water Content beneath the Mariana Arc. *Journal of Petrology*, 51(8): 1711—1738. https://doi.org/10.1093/petrology/egq036

Korsakov, A.V., Hermann, J., 2006. Silicate and Carbonate Melt Inclusions Associated with Diamonds in Deeply Subducted Carbonate Rocks. *Earth and Planetary Science Letters*, 241(1/2): 104—118. https://doi.org/10.1016/j.epsl.2005.10.037

Kotov, A.A., Smirnov, S.Z., Maksimovich, I.A., et al., 2017. Water in Melt Inclusions from Phenocrysts of Dacite Pumice of the Vetrovoy Isthmus (Iturup Island, Southern Kuriles). *IOP Conference Series: Earth and Environmental Science*, 110: 012009. https://doi.org/10.1088/1755-1315/110/1/012009

Labrousse, L., Jolivet, L., Agard, P., et al., 2002. Crustal-Scale Boudinage and Migmatization of Gneiss during Their Exhumation in the UHP Province of Western Norway. *Terra Nova*, 14(4): 263—270. https://doi.org/10.1046/j.1365-3121.2002.00422.x

Labrousse, L., Prouteau, G., Ganzhorn, A.C., 2011. Continental Exhumation Triggered by Partial Melting at Ultrahigh Pressure. *Geology*, 39(12): 1171—1174. https://doi.org/10.1130/g32316.1

Le Losq, C., Neuville, D., Moretti, R., et al., 2012. Determination of Water Content in Silicate Glasses Using Raman Spectrometry: Implications for the Study of Explosive Volcanism. *American Mineralogist*, 97(5/6): 779—790. https://doi.org/10.2138/am.2012.3831

Lee, C.T.A., Morton, D.M., Farner, M.J., et al., 2015. Field and Model Constraints on Silicic Melt Segregation by Compaction/Hindered Settling: The Role of Water and Its Effect on Latent Heat Release. *American Mineralogist*, 100(8/9): 1762—1777. https://doi.org/10.2138/am-2015-5121

Leschik, M., Heide, G., Frischat, G.H., et al., 2004. Determi-

nation of H_2O and D_2O Contents in Rhyolitic Glasses. *Physics and Chemistry of Glasses*, 45(4): 238－251.

Liebske, C., Behrens, H., Holtz, F., et al., 2003. The Influence of Pressure and Composition on the Viscosity of Andesitic Melts. *Geochimica et Cosmochimica Acta*, 67(3): 473－485. https://doi.org/10.1016/S0016-7037(02)01139-0

Liu, Q., Hermann, J., Zhang, J.F., 2013. Polyphase Inclusions in the Shuanghe UHP Eclogites Formed by Subsolidus Transformation and Incipient Melting during Exhumation of Deeply Subducted Crust. *Lithos*, 177: 91－109. https://doi.org/10.1016/j.lithos.2013.06.010

Liu, Q., Hermann, J., Zheng, S., et al., 2020. Evidence for UHP Anatexis in the Shuanghe UHP Paragneiss from Inclusions in Clinozoisite, Garnet and Zircon. *Journal of Metamorphic Geology*, 38(1): 129－155. https://doi.org/10.1111/jmg.12515

Long, D. A., 1977. Raman Spectroscopy. MacGraw-Hill, New York.

Mackwell, S.J., Kohlstedt, D.L., Paterson, M.S., 1985. The Role of Water in the Deformation of Olivine Single Crystals. *Journal of Geophysical Research*, 90(B13): 11319. https://doi.org/10.1029/jb090ib13p11319

Malaspina, N., Hermann, J., Scambelluri, M., et al., 2006. Polyphase Inclusions in Garnet-Orthopyroxenite (Dabie Shan, China) as Monitors for Metasomatism and Fluid-Related Trace Element Transfer in Subduction Zone Peridotite. *Earth and Planetary Science Letters*, 249(3/4): 173－187. https://doi.org/10.1016/j.epsl.2006.07.017

Mandeville, C.W., Webster, J.D., Rutherford, M.J., et al., 2002. Determination of Molar Absorptivities for Infrared Absorption Bands of H_2O in Andesitic Glasses. *American Mineralogist*, 87(7): 813－821. https://doi. org/10.2138/am-2002-0702

Massonne, H.J., 2001. First Find of Coesite in the Ultrahigh-Pressure Metamorphic Area of the Central Erzgebirge, Germany. *European Journal of Mineralogy*, 13(3): 565－570. https://doi. org/10.1127/0935-1221/2001/0013-0565

Massonne, H.J., Nasdala, L., 2003. Characterization of an Early Metamorphic Stage through Inclusions in Zircon of a Diamondiferous Quartzofeldspathic Rock from the Erzgebirge, Germany. *American Mineralogist*, 88(5－6): 883－889. https://doi.org/10.2138/am-2003-5-618

Matson, D.W., Sharma, S.K., Philpotts, J.A., 1986. Raman Spectra of some Tectosilicates and of Glasses along the Orthoclase-Anorthite and Nepheline-Anorthite Joins. *American Mineralogist*,71(5－6): 694－704.

McMillan, P.F., 1984. Structural Studies of Silicate Glasses and Melts-Applications and Limitations of Raman Spectroscopy. *American Mineralogist*, 69(6): 622－644.

McMillan, P.F., Hofmeister, A.M., 1988. Infrared and Raman Spectroscopy. *Mineralogical Society of America Reviews in Mineralogy*, 18(4): 99－159.

McMillan, P.F., Poe, B.T., Gillet, P.H., et al., 1994. A Study of SiO_2 Glass and Supercooled Liquid to 1 950 K via High-Temperature Raman Spectroscopy. *Geochimica et Cosmochimica Acta*, 58(17): 3653－3664. https://doi.org/10.1016/0016-7037(94)90156-2

McMillan, P.F., Remmele, J.R., 1986. Hydroxyl Sites in SiO_2 Glass: A Note on Infrared and Raman Spectra. *American Mineralogist*, 71: 772－778.

Mei, S., Kohlstedt, D.L., 2000. Influence of Water on Plastic Deformation of Olivine Aggregates: 2. Dislocation Creep Regime. *Journal of Geophysical Research*: *Solid Earth*, 105(B9): 21471－21481. https://doi. org/10.1029/2000jb900180

Mercier, M., Di Muro, A., Giordano, D., et al., 2009. Influence of Glass Polymerisation and Oxidation on Micro-Raman Water Analysis in Alumino-Silicate Glasses. *Geochimica et Cosmochimica Acta*, 73(1): 197－217. https://doi.org/10.1016/j.gca.2008.09.030

Mercier, M., Muro, A.D., Métrich, N., et al., 2010. Spectroscopic Analysis (FTIR, Raman) of Water in Mafic and Intermediate Glasses and Glass Inclusions. *Geochimica et Cosmochimica Acta*, 74(19): 5641－5656. https://doi.org/10.1016/j.gca.2010.06.020

Mikhno, A.O., Korsakov, A.V., 2013. K_2O Prograde Zoning Pattern in Clinopyroxene from the Kokchetav Diamond-Grade Metamorphic Rocks: Missing Part of Metamorphic History and Location of Second Critical End Point for Calc-Silicate System. *Gondwana Research*, 23(3): 920－930. https://doi.org/10.1016/j.gr.2012.07.020

Mikhno, A.O., Schmidt, U., Korsakov, A.V., 2013. Origin of K-Cymrite and Kokchetavite in the Polyphase Mineral Inclusions from Kokchetav UHP Calc-Silicate Rocks: Evidence from Confocal Raman Imaging. *European Journal of Mineralogy*, 25(5): 807－816. https://doi.org/10.1127/0935-1221/2013/0025-2321

Morgan, G.B., London, D., 1996. Optimizing the Electron Microprobe Analysis of Hydrous Alkali Aluminosilicate Glasses. *American Mineralogist*, 81(9/10): 1176－1185. https://doi.org/10.2138/am-1996-9-1016

Müller, A., Thomas, R., Wiedenbeck, M., et al., 2006a. Water Content of Granitic Melts from Cornwall and Erzgebirge: A Raman Spectroscopy Study of Melt Inclusions.

European Journal of Mineralogy, 18(4): 429－440. https://doi.org/10.1127/0935-1221/2006/0018-0429

Müller, D., Tesche, M., Eichler, H., et al., 2006b. Strong Particle Light Absorption over the Pearl River Delta (South China) and Beijing (North China) Determined from Combined Raman Lidar and Sun Photometer Observations. *Geophysical Research Letters*, 33(20): L20811. https://doi.org/10.1029/2006GL027196

Mysen, B.O., Holtz, F., Pichavant, M., et al., 1997. Solution Mechanisms of Phosphorus in Quenched Hydrous and Anhydrous Granitic Glass as a Function of Peraluminosity. *Geochimica et Cosmochimica Acta*, 61(18): 3913－3926. https://doi.org/10.1016/S0016-7037(97)00193-2

Mysen, B.O., Virgo, D., 1986a. Volatiles in Silicate Melts at High Pressure and Temperature. *Chemical Geology*, 57 (3/4): 333－358. https://doi. org/10.1016/0009-2541 (86)90057-4

Mysen, B.O., Virgo, D., 1986b. Volatiles in Silicate Melts at High Pressure and Temperature. *Chemical Geology*, 57 (3/4): 333－358. https://doi. org/10.1016/0009-2541 (86)90057-4

Mysen, B.O., Virgo, D., Scarfe, C.M., 1980. Relations between the Anionic Structure and Viscosity of Silicate Melts—A Raman Spectroscopic Study. *American Mineralogist*, 65: 690－710.

Mysen, B.O., Virgo, D., Seifert, F.A., 1982. The Structure of Silicate Melts: Implications for Chemical and Physical Properties of Natural Magma. *Reviews of Geophysics*, 20(3): 353－383. https://doi. org/10.1029/rg020i003p00353

Newman, S., Stolper, E.M., Epstein, S., 1986. Measurement of Water in Rhyolitic Glasses; Calibration of an Infrared Spectroscopic Technique. *American Mineralogist*, 71: 1527－1541.

Ni, H.W., Keppler, H., Behrens, H., 2011. Electrical Conductivity of Hydrous Basaltic Melts: Implications for Partial Melting in the Upper Mantle. *Contributions to Mineralogy and Petrology*, 162(3): 637－650. https://doi. org/10.1007/s00410-011-0617-4

Ni, H.W., Zhang, L., Guo, X., 2016. Water and Partial Melting of Earth's Mantle. *Science China Earth Sciences*, 59 (4): 720－730. https://doi. org/10.1007/s11430-015-5254-8

Ohlhorst, S., Behrens, H., Holtz, F., 2001. Compositional Dependence of Molar Absorptivities of Near-Infrared OH- and H_2O Bands in Rhyolitic to Basaltic Glasses. *Chemical Geology*, 174(1－3): 5－20. https://doi. org/10.1016/S0009-2541(00)00303-X

Regenauer-Lieb, K., Yuen, D.A., Branlund, J., 2001. The Initiation of Subduction: Criticality by Addition of Water? *Science*, 294(5542): 578－580. https://doi.org/10.1126/science.1063891

Rosenberg, C.L., Handy, M.R., 2005. Experimental Deformation of Partially Melted Granite Revisited: Implications for the Continental Crust. *Journal of Metamorphic Geology*, 23: 19－28.

Schiavi, F., Bolfan-Casanova, N., Withers, A.C., et al., 2018. Water Quantification in Silicate Glasses by Raman Spectroscopy: Correcting for the Effects of Confocality, Density and Ferric Iron. *Chemical Geology*, 483: 312－331. https://doi.org/10.1016/j.chemgeo.2018.02.036

Severs, M.J., Azbej, T., Thomas, J.B., et al., 2007. Experimental Determination of H_2O Loss from Melt Inclusions during Laboratory Heating: Evidence from Raman Spectroscopy. *Chemical Geology*, 237(3/4): 358－371. https://doi.org/10.1016/j.chemgeo.2006.07.008

Sharma, S.K., Mammone, J.F., Nicol, M.F., 1981. Raman Investigation of Ring Configurations in Vitreous Silica. *Nature*, 292(5819): 140－141. https://doi. org/10.1038/292140a0

Shaw, A.M., Hauri, E.H., Fischer, T.P., et al., 2008. Hydrogen Isotopes in Mariana Arc Melt Inclusions: Implications for Subduction Dehydration and the Deep-Earth Water Cycle. *Earth and Planetary Science Letters*, 275 (1－2): 138－145. https://doi. org/10.1016/j.epsl.2008.08.015

Silver, L.A., Ihinger, P.D., Stolper, E., 1990. The Influence of Bulk Composition on the Speciation of Water in Silicate Glasses. *Contributions to Mineralogy and Petrology*, 104(2): 142－162. https://doi. org/10.1007/BF00306439

Song, S.G., Yang, J.S., Xu, Z., et al., 2003. Metamorphic Evolution of the Coesite-Bearing Ultrahigh-Pressure Terrane in the North Qaidam, Northern Tibet, NW China. *Journal of Metamorphic Geology*, 21(6): 631－644. https://doi.org/10.1046/j.1525-1314.2003.00469.x

Sorby, H.C., 1858. On the Microscopical, Structure of Crystals, Indicating the Origin of Minerals and Rocks. *Quarterly Journal of the Geological Society*, 14(1/2): 453－500. https://doi.org/10.1144/gsl.jgs.1858.014.01-02.44

Stepanov, A.S., Hermann, J., Korsakov, A.V., et al., 2014. Geochemistry of Ultrahigh-Pressure Anatexis: Fractionation of Elements in the Kokchetav Gneisses during Melting at Diamond-Facies Conditions. *Contributions to Mineralogy and Petrology*, 167(5): 1002. https://doi.org/10.1007/s00410-014-1002-x

Stepanov, A.S., Hermann, J., Rubatto, D., et al., 2016. Melting History of an Ultrahigh-Pressure Paragneiss Revealed by Multiphase Solid Inclusions in Garnet, Kokchetav Massif, Kazakhstan. *Journal of Petrology*, 57(8): 1531－1554. https://doi. org/10.1093/petrology/egw049

Stolper, E., 1982. Water in Silicate Glasses: An Infrared Spectroscopic Study. *Contributions to Mineralogy and Petrology*, 81(1): 1－17. https://doi. org/10.1007/BF00371154

Tacchetto, T., Bartoli, O., Cesare, B., et al., 2018. Multiphase Inclusions in Peritectic Garnet from Granulites of the Athabasca Granulite Terrane (Canada): Evidence of Carbon Recycling during Neoarchean Crustal Melting. *Chemical Geology*, 508: 197－209. https://doi. org/10.1016/j.chemgeo.2018.05.043

Thomas, R., 2000. Determination of Water Contents of Granite Melt Inclusions by Confocal Laser Raman Microprobe Spectroscopy. *American Mineralogist*, 85(5－6): 868－872. https://doi.org/10.2138/am-2000-5-631

Thomas, R., 2002. Determination of Water Contents in Melt Inclusions by Laser Raman Spectroscopy. Workshop-Short Course on Volcanic Systems, Geochemical and Geophysical Monitoring. In: De Vivo, B., Bodnar, R. J., eds., Melt Inclusions: Methods, Applications and Problems. Seiano di Vico Equense (Napoli), Italy, Proceedings, 211－216.

Thomas, R., Davidson, P., 2012. Water in Granite and Pegmatite-Forming Melts. *Ore Geology Reviews*, 46: 32－46. https://doi. org/10.1016/j. oregeorev.2012.02.006

Thomas, R., Kamenetsky, V. S., Davidson, P., 2006. Laser Raman Spectroscopic Measurements of Water in Unexposed Glass Inclusions. *American Mineralogist*, 91(2－3): 467－470. https://doi.org/10.2138/am.2006.2107

Thomas, S.M., Thomas, R., Davidson, P., et al., 2008. Application of Raman Spectroscopy to Quantify Trace Water Concentrations in Glasses and Garnets. *American Mineralogist*, 93(10): 1550－1557. https://doi. org/10.2138/am.2008.2834

Venugopal, S., Schiavi, F., Moune, S., et al., 2020. Melt Inclusion Vapour Bubbles: The Hidden Reservoir for Major and Volatile Elements. *Scientific Reports*, 10: 9034. https://doi.org/10.1038/s41598-020-65226-3

Wallace, P. J., 2005. Volatiles in Subduction Zone Magmas: Concentrations and Fluxes Based on Melt Inclusion and Volcanic Gas Data. *Journal of Volcanology and Geothermal Research*, 140(1/2/3): 217－240. https://doi.org/10.1016/j.jvolgeores.2004.07.023

Wallis, S., Tsuboi, M., Suzuki, K., et al., 2005. Role of Partial Melting in the Evolution of the Sulu (Eastern China) Ultrahigh-Pressure Belt. *Geology*, 33(2): 129－132. https://doi.org/10.1130/G20991.1

Wang, D., Lu, H.Z., Shan, Q., 2017. Advances on Melt Inclusion Studies. *Acta Petrologica Sinica*, 33(2): 653－666 (in Chinese with English abstract).

Wang, L., Kusky, T.M., Polat, A., et al., 2014. Partial Melting of Deeply Subducted Eclogite from the Sulu Orogen in China. *Nature Communications*, 5: 5604. https://doi.org/10.1038/ncomms6604

Wang, S.J., Wang, L., Brown, M., et al., 2017. Fluid Generation and Evolution during Exhumation of Deeply Subducted UHP Continental Crust: Petrogenesis of Composite Granite-Quartz Veins in the Sulu Belt, China. *Journal of Metamorphic Geology*, 35(6): 601－629. https://doi.org/10.1111/jmg.12248

Wang, X. C., Li, Q. L., Wilde, S. A., et al., 2021. Decoupling between Oxygen and Radiogenic Isotopes: Evidence for Generation of Juvenile Continental Crust by Partial Melting of Subducted Oceanic Crust. *Journal of Earth Science*, 32(5): 1212－1225. https://doi. org/10.1007/s12583-020-1095-2

Withers, A. C., Behrens, H., 1999. Temperature-Induced Changes in the NIR Spectra of Hydrous Albitic and Rhyolitic Glasses between 300 and 100 K. *Physics and Chemistry of Minerals*, 27(2): 119－132. https://doi.org/10.1007/s002690050248

Yang, J. J., Godard, G., Smith, D. C., 1998. K-Feldspar-Bearing Coesite Pseudomorphs in an Eclogite from Lanshantou (Eastern China). *European Journal of Mineralogy*, 10(5): 969－986. https://doi.org/10.1127/ejm/10/5/0969

Yoshino, T., Matsuzaki, T., Yamashita, S., et al., 2006. Hydrous Olivine Unable to Account for Conductivity Anomaly at the Top of the Asthenosphere. *Nature*, 443 (7114): 973－976. https://doi.org/10.1038/nature05223

Zack, T., John, T., 2007. An Evaluation of Reactive Fluid Flow and Trace Element Mobility in Subducting Slabs. *Chemical Geology*, 239(3/4): 199－216. https://doi.org/10.1016/j.chemgeo.2006.10.020

Zajacz, Z., Halter, W., Malfait, W.J., et al., 2005. A Composition-Independent Quantitative Determination of the Water Content in Silicate Glasses and Silicate Melt Inclusions by Confocal Raman Spectroscopy. *Contributions to Mineralogy and Petrology*, 150(6): 631－642. https://doi.org/10.1007/s00410-005-0040-9

Zeng, L. S., Chen, Z. Y., Chen, J., 2013. Metamorphic Solid Salt (KCl-NaCl) in Quartzo-Feldspathic Polyphase Inclusions in the Sulu Ultrahigh-Pressure Eclogite. *Chinese Science Bulletin*, 58(8): 931－937. https://doi.org/10.1007/s11434-012-5373-y

Zeng, L. S., Liang, F. H., Asimow, P., et al., 2009. Partial Melting of Deeply Subducted Continental Crust and the Formation of Quartzofeldspathic Polyphase Inclusions in the Sulu UHP Eclogites. *Chinese Science Bulletin*, 54(15): 2580－2594. https://doi. org/10.1007/s11434-009-0426-6

Zhang, J. F., Green, H. W., Bozhilov, K., et al., 2004. Faulting Induced by Precipitation of Water at Grain Boundaries in Hot Subducting Oceanic Crust. *Nature*, 428(6983): 633－636. https://doi.org/10.1038/nature02475

Zhang, R., Liou, J., Iizuka, Y., et al., 2009. First Record of K-Cymrite in North Qaidam UHP Eclogite, Western China. *American Mineralogist*, 94(2/3): 222－228. https://doi.org/10.2138/am.2009.2983

Zhang, Y. X., Ni, H. W., Chen, Y., 2010. Diffusion Data in Silicate Melts. *Reviews in Mineralogy and Geochemistry*, 72(1): 311－408. https://doi.org/10.2138/rmg.2010.72.8

Zhang, Z. M., Shen, K., Sun, W. D., et al., 2008. Fluids in Deeply Subducted Continental Crust: Petrology, Mineral Chemistry and Fluid Inclusion of UHP Metamorphic Veins from the Sulu Orogen, Eastern China. *Geochimica et Cosmochimica Acta*, 72(13): 3200－3228. https://doi.org/10.1016/j.gca.2008.04.014

Zheng, Y. F., Ye, K., 2009. Developing the Plate Tectonics from Oceanic Subduction to Continental Collision. *Chinese Science Bulletin*, 54(13): 1799－1803.

Zheng, Y. F., 2009. Fluid Regime in Continental Subduction Zones: Petrological Insights from Ultrahigh-Pressure Metamorphic Rocks. *Journal of the Geological Society*, 166(4): 763－782. https://doi. org/10.1144/0016-76492008-016R

Zheng, Y. F., 2012. Metamorphic Chemical Geodynamics in Continental Subduction Zones. *Chemical Geology*, 328: 5－48. https://doi.org/10.1016/j.chemgeo.2012.02.005

Zheng, Y. F., 2019. Subduction Zone Geochemistry. *Geoscience Frontiers*, 10(4): 1223－1254. https://doi. org/10.1016/j.gsf.2019.02.003

Zheng, Y. F., Chen, Y. X., 2019. Crust-Mantle Interaction in Continental Subduction Zones. *Earth Science*, 44(12): 3961－3983(in Chinese with English abstract).

Zheng, Y. F., Gao, P., 2021. The Production of Granitic Magmas through Crustal Anatexis at Convergent Plate Boundaries. *Lithos*, 402/403: 106232. https://doi.org/10.1016/j.lithos.2021.106232

Zheng, Y. F., Hermann, J., 2014. Geochemistry of Continental Subduction-Zone Fluids. *Earth, Planets and Space*, 66(1): 93. https://doi.org/10.1186/1880-5981-66-93

Zheng, Y. F., Xia, Q. X., Chen, R. X., et al., 2011. Partial Melting, Fluid Supercriticality and Element Mobility in Ultrahigh-Pressure Metamorphic Rocks during Continental Collision. *Earth-Science Reviews*, 107(3/4): 342－374. https://doi.org/10.1016/j.earscirev.2011.04.004

附中文参考文献

高晓英,2019. 大陆俯冲带大规模的变质流体活动:来自大别造山带超高压硬玉石英岩的记录. 地球科学, 44(12): 4064－4071.

王蝶,卢焕章,单强,2017. 岩浆熔体包裹体研究进展. 岩石学报, 33(2): 653－666.

郑永飞,陈伊翔,2019. 大陆俯冲带壳幔相互作用. 地球科学, 44(12): 3961－3983.